Microsecond Rotational Dynamics of Spin-Labeled Ca-ATPase during Enzymatic Cycling Initiated by Photolysis of Caged ATP[†]

Scott M. Lewis and David D. Thomas*

Department of Biochemistry, University of Minnesota Medical School, Minneapolis, Minnesota 55455
Received February 6, 1991; Revised Manuscript Received May 24, 1991

ABSTRACT: We have measured the microsecond rotational motions of the sarcoplasmic reticulum (SR) Ca-ATPase as a function of enzyme-specific ligands, including those that induce active calcium transport. We labeled the Ca-ATPase with a maleimide spin probe and detected rotational dynamics using saturation-transfer electron paramagnetic resonance (ST-EPR). This probe's ST-EPR spectra have been shown to be sensitive to microsecond protein rotational motion, corresponding to large-scale protein rotations that should be affected by changes in the enzyme's shape, flexibility, protein–protein interactions (oligomeric state), and protein–lipid interactions. We found that the motions of the enzyme–nucleotide and the enzyme–nucleotide/Ca states are indistinguishable from the motions in the absence of ligands. Rotational mobility does decrease in response to the addition of DMSO, a solvent that inhibits Ca-ATPase activity and stabilizes the phosphoenzyme. However, the addition of phosphate to form phosphoenzyme, in the presence or absence of DMSO, does not change the motions significantly. During the steady state of active calcium transport, the microsecond rotational mobility is indistinguishable from that of the resting enzyme. In order to detect any transient changes in mobility that might not be detectable in the steady state and to improve the precision of steady-state measurements, we photolyzed caged ATP with a laser pulse in the presence of calcium and detected the ST-EPR response from the spin-labeled enzyme, with a time resolution of 1 s. No significant change in the ST-EPR signal was observed, indicating that the effective rotational correlation time does not change by more than 10% in the transient or steady-state phases of the Ca-ATPase cycle. While protein motion has been shown to be important to the function of the Ca-ATPase, this study indicates that changes in the microsecond protein rotational mobility, which would be caused by changes in the enzyme's shape, flexibility, oligomeric state, or protein–lipid interactions, do not occur as part of the calcium transport cycle. This does not rule out (1) transient-phase effects lasting less than 1 s, (2) short-lived effects that occur after the rate-limiting transition, or (3) rearrangements within an oligomeric unit that do not affect the overall rotational mobility.

Tʜe intrinsic membrane protein responsible for the transport of calcium into the sarcoplasmic reticulum (SR)[1] is the Ca-ATPase. While it has been shown that the Ca-ATPase requires microsecond rotational mobility for normal function (Thomas & Hidalgo, 1978; Squier et al., 1988a,b), several questions remain concerning the molecular dynamics of the Ca-ATPase transport cycle. In particular, it has been proposed that changes in the enzyme's shape, flexibility, or protein–protein interactions play a functional role in the kinetic cycle [reviewed by Martonosi et al. (1990)].

One type of protein–protein interaction that could play a functional role is the oligomeric association of Ca-ATPase monomers into dimers or tetramers (Martonosi & Beeler, 1983). Electron microscopy (Deamer & Baskin, 1969; Jilka et al., 1975; Scales & Inesi, 1976) and fluorescence energy transfer (Vanderkooi et al., 1977; Papp et al., 1987) have both suggested the presence of oligomers. Using freeze-fracture electron microscopy in conjunction with optical diffraction analysis of the micrographs, Napolitano et al. (1983) concluded that the Ca-ATPase forms a dimer in the membrane. However, Highsmith and Cohen (1987) concluded that the fluorescein isothiocyanate labeled Ca-ATPase is probably a tetramer. Fagan and Dewey (1986), using resonance energy

transfer, reported that the degree of oligomerization was temperature dependent and that the enzyme was tetrameric at temperatures less than 5 °C. Using chemical cross-linking of the Ca-ATPase monomers, Squier et al. (1988b) concluded that although protein–protein interactions occur, no specific and stable oligomeric complexes exist.

The functional importance of these protein interactions has been addressed through the study of putative intermediates in the transport cycle, notably the vanadate-inhibited enzyme. Vanadate is proposed to bind in place of inorganic phosphate and inhibit the reaction cycle (O'Neal et al., 1979; Dupont & Bennett, 1982; Ortiz et al., 1984; Varga et al., 1985). Electron microscopy (Dux & Martonosi, 1983) showed that vanadate induced two-dimensional arrays of Ca-ATPase proteins within the membrane, although later studies suggested that only the higher oligomers of vanadate, especially deca-

---

[1] Abbreviations: SR, sarcoplasmic reticulum; EPR, electron paramagnetic resonance; ST-EPR, saturation-transfer EPR; MSL, *N*-(1-oxy-2,2,6,6-tetramethyl-4-piperidinyl)maleimide; IASL, *N*-(1-oxy-2,2,6,6-tetramethyl-4-piperidinyl)iodoacetamide; IAEDANS, 5-[[2-[(iodoacetyl)amino]ethyl]amino]naphthalene-1-sulfonic acid; FITC, fluorescein 5-isothiocyanate; SRB, sarcoplasmic reticulum buffer; V_i, vanadate; EGTA, ethylene glycol bis(β-aminoethyl ether)-*N*,*N*,*N′*,*N′*-tetraacetic acid; DMSO, dimethyl sulfoxide; P_i, inorganic phosphate; AMPPNP, adenosine 5′-(β,γ-iminotriphosphate); caged ATP, adenosine 5′-triphosphate P^3-1-(2-nitrophenyl)ethyl ester; DSP, dithiobis(succinimido propionate); MES, 2-(*N*-morpholino)ethanesulfonic acid; MOPS, 3-(*N*-morpholino)propanesulfonic acid.

vanadate, promoted array formation (Maurer & Fleischer, 1984; Lewis & Thomas, 1986). The basic unit within these vanadate-induced arrays was found to be a dimer (Buhle et al., 1983; Taylor et al., 1984). Lewis and Thomas (1986) found that decavanadate decreased the rotational mobility of the Ca-ATPase in native membranes, consistent with array formation, whereas monovanadate did not. Markus et al. (1989) concluded that protein–protein interactions were not involved in calcium and monovanadate binding to a fluorescein isothiocyanate labeled Ca-ATPase.

Since vanadate binding to the Ca-ATPase is proposed to produce a phosphoenzyme analogue, the decavanadate-induced array suggests that the phosphoenzyme is a dimer. Dux et al. (1985) found that arrays formed under conditions designed to mimic the unphosphorylated enzyme contain monomers as the unit structure and proposed that enzyme phosphorylation involves a monomer-to-dimer transition. Myotoxin a, reported to inhibit calcium translocation, disrupts decavanadate-induced arrays, suggesting that the inhibitory mechanism is protein dissociation (Volpe et al., 1986). Squier and Thomas (1988) concluded that protein rotational mobility was essential for phosphoenzyme decomposition, the rate-limiting step in the Ca-ATPase reaction cycle. Protein–protein interactions have also been implicated in Mg sensitivity of phosphoenzyme decomposition (Yantorno et al., 1983) and in calcium cooperativity (Watanabe et al., 1981).

Other studies have concerned the effects of ATP on protein–protein interactions. Studies on the ADP-sensitive and -insensitive phosphoenzymes, $E_1 \sim P \cdot Ca_2$ and $E_2 - P \cdot Ca_2$, respectively, have concluded that the kinetics require a dimer with interacting subunits (Froehlich & Heller, 1985; Wang, 1986). Using HPLC techniques, Andersen and Vilsen (1985) found that the Ca-ATPase existed in an equilibrium between monomers, dimers, and higher oligomers in the presence of detergent. Under these conditions, ATP, vanadate, and phosphoenzyme turnover promoted a shift toward monomers. However, enzyme phosphorylation by ATP had no effect on interprotein energy transfer in the absence of detergent, suggesting that no changes occur in the native membrane (Inesi & Watanabe 1982). Hymel et al. (1984), using radiation inactivation/target size analysis, concluded that the Ca-ATPase is a constant dimer unaffected by phosphoenzyme formation. Monomeric Ca-ATPase, obtained by detergent solubilization, forms ADP-insensitive phosphoenzyme and binds ATP and vanadate (Andersen et al., 1986). McIntosh and Ross (1988) found that monomeric Ca-ATPase, also obtained by detergent solubilization, could be phosphorylated by inorganic phosphate and then catalyze calcium-dependent ATP synthesis from ADP, suggesting that oligomeric association was not necessary for function.

In order to determine whether functional changes occur in the degree of protein association, the Ca-ATPase must be monitored in its native membrane without detergent. In addition, it must be studied under physiological conditions while active calcium transport is occurring. Saturation-transfer electron paramagnetic resonance spectroscopy (ST-EPR; Thomas & Hidalgo, 1978; Thomas, 1986; Squier & Thomas, 1986a,b) has been shown to be sensitive to microsecond rotational motion of the Ca-ATPase, corresponding to large-scale protein rotations that are slowed by increased protein association (Lewis & Thomas, 1986; Squier & Thomas, 1988). In the present study, we have used ST-EPR to monitor microsecond protein mobility under physiological conditions, including active calcium transport. In order to detect possible changes in protein motion during the transient phase of the

Ca-ATPase reaction cycle, the EPR signal was detected continuously before and after the laser flash photolysis of caged ATP.

MATERIALS AND METHODS

Preparation of SR Vesicles. Sarcoplasmic reticulum (SR) vesicles were prepared from the white (fast) skeletal muscle of New Zealand white rabbits according to the method of Fernandez et al. (1980). The SR was suspended in sucrose buffer (0.3 M sucrose and 20 mM MOPS, pH 7.0) at a concentration of 20–40 mg/mL protein, rapidly frozen, and stored in liquid nitrogen until use.

Solutions. All experiments were performed in a solution of 0.1 M KCl, 10 mM imidazole, 0.5 mM EGTA, and 5 mM $MgCl_2$, pH 7.4 (Dux & Martonosi, 1983a), designated SR buffer (SRB), unless otherwise specified. All vanadate solutions were made from Na_3VO_4 obtained from Fischer Scientific Company. Stock solutions of monovanadate and decavanadate were prepared according to Dux and Martonosi (1983a) and Varga et al. (1985). The solutions were characterized according to Lewis and Thomas (1986). In the discussions that follow, vanadate concentrations are given in terms of the total moles of vanadate present without correction for polymerization. AMPPNP was obtained from Sigma Chemical Co. Caged ATP solutions (gift from Dr. Y. Goldman) were stored in the dark in liquid nitrogen until use.

Protein Assay. Protein concentrations were determined by the biuret assay, with bovine serum albumin as a standard (Gornall et al., 1949). The Ca-ATPase content of the total SR protein was assayed by densitometer scans of Coomassie-stained gels of the SR preparation according to the method of Bigelow et al. (1986). The SR Ca-ATPase content was found to be 78 ± 5% (by weight).

Lipid-to-Protein Ratio. The lipid-to-protein ratio was calculated as the moles of phospholipid [determined by the method of Chen et al. (1956)] divided by the moles of Ca-ATPase (calculated by multiplying the protein concentration by the fraction of Ca-ATPase present, determined by gel electrophoresis, and dividing by a molecular mass of 115 kDa). The ratio found was 75 ± 5.

ATPase Activity. ATPase activities were measured by determining the rate of steady-state phosphate liberation in the presence of 5 mM MgATP, by using an assay for inorganic phosphate essentially as described by Lanzetta et al. (1977). Activity was measured with and without calcium and ionophore. The protein concentration was 0.05 mg/mL unless otherwise specified. The amount of added ionophore, A23187, was calibrated for each preparation of SR in order to ensure full activation of activity. This was usually 1 μg/0.05 mg of SR protein. The reaction was started by the addition of 5 mM ATP. Sequential aliquots of the reaction mixture were quenched, and the absorbance was read at 660 nm and compared to a phosphate standard to determine phosphate released from ATP. The activity was 2.1 ± 0.1 μmol/(min·mg of protein) and 0.05 ± 0.01 μmol/(min·mg of protein) at 25 and 4 °C, respectively. This gives a turnover number of 0.1 s^{-1} at 4 °C. Enzyme activity was unaffected (less than 5% difference from control) by the label (Bigelow et al., 1986).

Phosphoenzyme Formation. The phosphoenzyme formed from inorganic phosphate was assayed essentially according to the procedure of Barrabin et al. (1984). $H_3{}^{32}PO_4$ was obtained from New England Nuclear. The assay tubes contained 100 μg of SR protein in the phosphorylation buffer (variable). Inorganic phosphate (containing ^{32}P) was added to produce a concentration of 5 mM. After 10 min of incubation, the reaction was quenched with 0.125 M perchloric

acid and 4 mM cold inorganic phosphate. The solution was filtered through a 0.45-μm Millipore filter, and the filter was washed with ice-cold perchloric acid and phosphate. The filter was then counted in a scintillation counter. A background blank (prepared in the same way as the assay tube except it was quenched before phosphate was added) was subtracted from the assay value. This was related to bound phosphate by counting an aliquot of the unfiltered solution. Phospho-enzyme was quantitated by dividing moles of P_i bound by moles of Ca-ATPase, taking into account the percentage of the SR protein that was the Ca-ATPase.

Cross-Linking. Cross-linking of the EPR samples was done as described by Kurobe et al. (1983) and modified by Squier et al. (1988b). The Ca-ATPase was cross-linked by the ho-mobifunctional reagent dithiobis(succinimido propionate) (DSP). In a medium of 0.3 M sucrose, 1.01 mM $CaCl_2$, 1.00 mM EGTA, and 20 mM MOPS, pH 7.0, the reaction was started by the addition of 0.1 M DSP to a concentration of 5 mM with a protein concentration of 4 mg/mL. This was incubated at 22 °C for 5 min. The reaction was terminated by the addition of glycine to a concentration of 91 mM. The SR was subsequently washed in sucrose buffer as described previously.

Spin-Labeling. The Ca-ATPase was labeled with a male-imide spin label, N-(1-oxyl-2,2,6,6-tetramethyl-4-piperidinyl)maleimide, designated MSL (obtained from Ald-rich Chemical Co.), according to the procedure of Bigelow et al. (1986). Spectral changes that were observed for this preparation were consistent with changes in overall mobility (Squier et al., 1988b). This results in a stoichiometry of 1.7 mol of spin label/mol of Ca-ATPase (Bigelow et al., 1986). Analysis of both labeling kinetics (Hidalgo & Thomas, 1977) and the spin distribution on tryptic peptides indicated that the spin label was attached to more than one site.

EPR Sample Preparation. Samples were suspended in the appropriate buffer by centrifuging in that buffer minus EGTA for 45 min at 100000g. The pellets were resuspended in the buffer plus EGTA (if appropriate). Ligand additions were made to the resuspended sample. Mono- and decavanadate EPR samples were prepared by incubation of 30–40 mg/mL protein with 5 mM monovanadate or decavanadate for 1 day at pH 7.4 in SRB.

EPR Spectral Acquisition. EPR spectra were obtained with a Varian E-109 EPR spectrometer interfaced to a Northstar computer, following the procedures described in detail by Squier and Thomas (1986a,b). Samples were placed in a capillary made from the gas-permeable plastic TPX, (Bigelow et al., 1986) and deoxygenated with N_2 for 20 min prior to scanning, since it has previously been shown that O_2 affects ST-EPR spectra (Squier & Thomas, 1986a). Conventional EPR spectra, which are sensitive to nanosecond motions and are designated V_1, were obtained with 100-kHz field modu-lation (with a modulation amplitude of 2.0 G) and a microwave field amplitude of 0.14 G. This microwave intensity usually produces slight saturation with MSL-SR but does not distort the line shape significantly. ST-EPR spectra, which are sensitive to microsecond motions, are designated V_2'. Spectra were obtained with 50-kHz field modulation (with a modu-lation amplitude of 5 G) and a microwave field amplitude of 0.25 G. The 100-kHz reference was set 90° out-of-phase by minimizing the signal in the absence of saturation (microwave field amplitude of 0.032 G).

In experiments involving caged ATP, spectra were acquired as above except that a Bruker ER 200D EPR Spectrometer was used. A Lambda Physik EMG 53 MSC XeCl excimer

laser was used to release the ATP by directing the beam (308 nm) through radiation slits into the EPR cavity (Bruker ER4102). The surface of the quartz temperature control dewar was roughened with diamond paste to ensure uniform distribution of light over the sample, as verified with photo-sensitive film. The sample, in a 50-μL quartz flat cell (0.5-mm path length), was positioned in the beam and 20–30% of the 5 mM caged ATP was converted to ATP by a 1-s burst of 50 pulses, each of which had an energy density of about 5 mJ/cm^2. The ATPase activity was determined before and after the laser pulse by using the assay described above.

EPR Spectral Analysis. Conventional EPR spectra were characterized by the spectral parameters W/S, Δ_L, and $2T_\parallel'$ (see Figure 1). W/S is the ratio of the second ("weakly immobilized") to the first ("strongly immobilized") low-field peak, Δ_L is the outer half-width at half-height of the low-field peak, and $2T_\parallel'$ is the splitting between the outer extrema of the spectrum. ST-EPR spectra were characterized by spectral parameters as defined by Squier and Thomas (1986a). These included the line shape parameters L''/L, C'/C, H''/H (see Figure 1), and L''/L_{in}. L_{in} is the line height of the in-phase low-field peak recorded at $^1/_{10}$ gain. An integrated intensity parameter was measured from the integral of the V_2' spectrum divided by the gain normalized to the number of spins (the double integral of the V_1 spectrum divided by the gain). The V_1 double integral was obtained from the spectrum recorded at 0.14 G, multiplied by the ratio of the line heights of the center-field peaks recorded at 0.032 and 0.14 G. The result is an integrated intensity parameter equivalent to that defined by Squier and Thomas (1986a). Protein rotational motion was then characterized by the effective rotational correlation time, τ_r, determined by comparing the value of V_2' spectral param-eters with calibration plots of these parameters obtained from spin-labeled hemoglobin in aqueous glycerol solutions where the correlation times can be calculated from theory (Squier & Thomas, 1986a,b). Hemoglobin undergoes isotropic motion, while the motion for the Ca-ATPase is more complex (Thomas, 1986; Birmachu & Thomas, 1990). Therefore the calculated correlation times are effective correlation times, probably corresponding to upper bounds for the actual cor-relation times (Thomas, 1986).

Except in cases where individual parameters are noted, the ST-EPR results cited in the tables and text were calculated in the following way. For each parameter an effective cor-relation time was calculated. This time was divided by the control time obtained from the same parameter in the control spectrum, corresponding to no ligand addition. The ratios from the five parameters were then averaged so that one number was obtained for each experimental condition. These nor-malized correlation times were then averaged for all identical experiments. Unless otherwise indicated, the relative corre-lation times thus obtained were not significantly different from those obtained from individual spectral parameters.

RESULTS

Comparison of the Effects of Cross-Linking and Deca-vanadate. Previous experiments with the cross-linker DSP have shown that the ST-EPR spectrum of MSL-Ca-ATPase is sensitive to changes in the oligomeric state (Squier et al., 1988b). The cross-linking conditions described under Mate-rials and Methods resulted in maximal cross-linking, i.e., monomers were no longer detected on sodium dodecyl sul-fate–polyacrylamide gels (Squier et al., 1988b). It is of interest to know whether the two methods of decreasing protein mo-bility, cross-linking and decavanadate, affect protein mobility to the same extent. DSP increased the effective correlation

Table I: Effects of Cross-Linking and/or Decavanadate[a]

	−decavanadate	+decavanadate
−cross-linking	1	1.55 ± 0.21
+cross-linking	1.87 ± 0.17	2.57 ± 0.31

[a]The values shown are τ_r/τ_{r0}, where τ_r is the effective rotational correlation time (from ST-EPR) under the given conditions, and τ_{r0} is the time measured in the absence of cross-linking and decavanadate (see Materials and Methods). All experiments were performed in SRB at 4 °C. Decavanadate was added to a final concentration of 5 mM and incubated as described under Materials and Methods. Cross-linking was obtained with DSP as described under Materials and Methods. For the sample treated with both treatments, the decavanadate incubation was done before cross-linking. The mean control correlation time was 55 ± 8 μs. The uncertainty is the standard error of the mean.
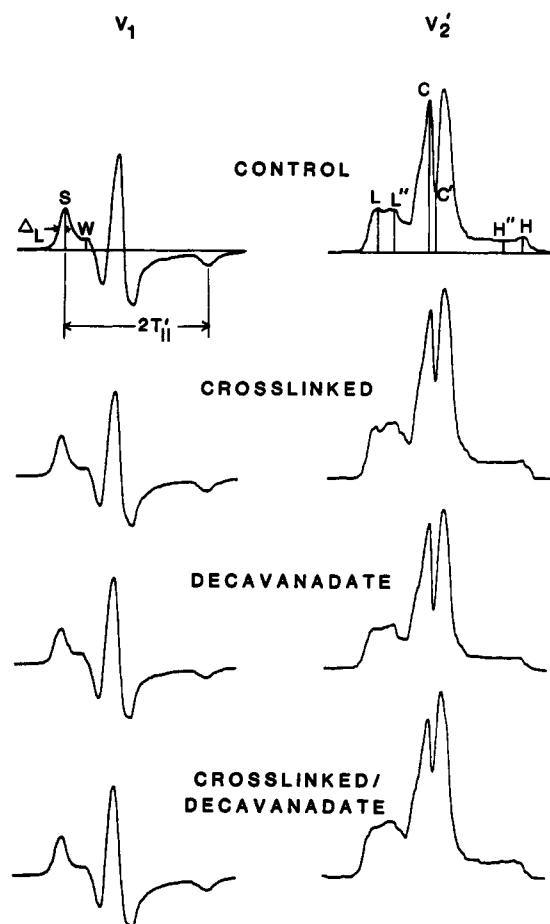

FIGURE 1: Effects of cross-linking and decavanadate on EPR spectra of MSL-Ca-ATPase. Left: conventional EPR spectra (V_1). Right: saturation-transfer EPR spectra (V_2'). The spectral parameters are ilustrated on the control spectra in row 1. Rows 2 and 4: cross-linked with DSP. Rows 3 and 4: treated with 5 mM decavanadate at least 1 h before data acquisition or cross-linking. Effective rotational correlation times determined from the ST-EPR spectra are given in Table I. Spectra were recorded at 4 °C. The baseline is 110 G wide.

times of the protein rotational motion by a greater extent than decavanadate (87% to 55%, see Table I), and the two effects together (157%) were greater than either one individually (see Figure 1 and Table I). The time scale for the decavanadate effect was determined by monitoring C'/C and the integral parameter versus time. We found that the complete decavanadate effect was obtained within 30–40 min following decavanadate addition at 4 °C. The value of the effective correlation time did not change further following 24 h of incubation at 4 °C. The average increase in the correlation time was 63 ± 6%.

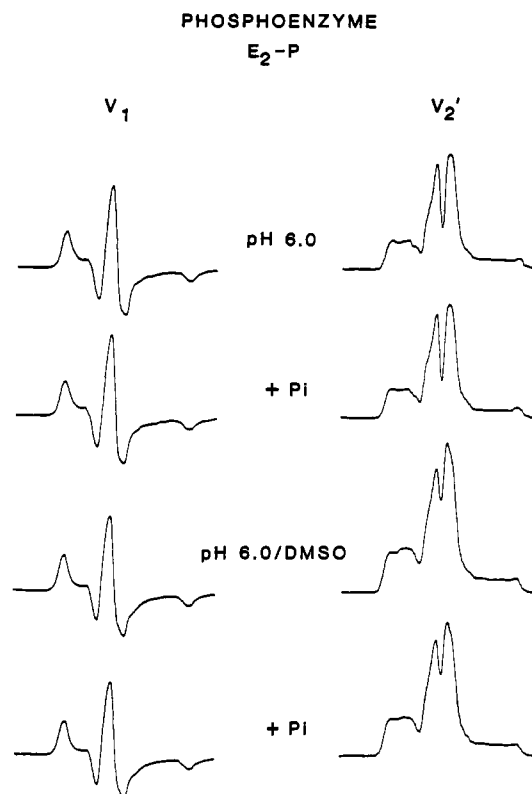*Effects of Phosphoenzyme Formation.* The phosphoenzyme levels formed from inorganic phosphate at 25 °C were as

FIGURE 2: Effects of phosphoenzyme formation on EPR spectra of MSL-Ca-ATPase. Left: conventional EPR spectra (V_1). Right: saturation-transfer EPR spectra (V_2'). All solutions contained 2 mM EGTA, 10 mM MgCl$_2$, and 30 mM MES (pH 6.0). Rows 1 and 2: no DMSO. Rows 3 and 4: 40% DMSO. Rows 2 and 4: 5 mM potassium phosphate. Effective rotational correlation times determined from the ST-EPR spectra are given in Table II. Spectra were recorded at 4 °C. The baseline is 110 G wide.

Table II: Effects of Phosphoenzyme Formation at pH 6.0[a]

	−KCl		+KCl
	4 °C	25 °C	25 °C
phosphoenzyme	0.95 ± 0.010	0.91 ± 0.11	1.01 ± 0.11
DMSO	2.54 ± 0.56	1.51 ± 0.38	1.74 ± 0.35
phosphoenzyme/DMSO	0.84 ± 0.06	1.00 ± 0.09	0.91 ± 0.08

[a]Values shown are τ_r/τ_{r0} (see Materials and Methods), where τ_r and τ_{r0} are the effective rotational correlation times (from ST-EPR) in the presence and absence of the added ligand (phosphate for the phosphoenzyme, DMSO for the DMSO results, and phosphate for the phosphoenzyme/DMSO results with τ_{r0} being the correlation times from the DMSO spectrum). All solutions contained 10 mM MgCl$_2$, 2 mM EGTA, and 30 mM MES at pH 6.0. "Phosphoenzyme" indicates the presence of 5 mM phosphate. "+KCl" indicates the presence of 80 mM KCl. "DMSO" indicates the presence of 40% DMSO (v/v). The mean control correlation times were 55 ± 8, 22 ± 5, and 27 ± 4 μs for columns 1, 2, and 3, respectively. Each value in the table is the mean of the ratios from 2–6 experiments, and the uncertainty is the standard deviation.

follows (expressed as mol of phosphoenzyme/mol of Ca-ATPase): (1) 0.32 ± 0.05 in a buffer of mM KH$_2$PO$_4$, 2 mM EGTA, 10 mM MgCl$_2$, and 30 mM MES, pH 6.0, and (2) 0.59 ± 0.05 in the same solution plus 40% DMSO. The addition of 80 mM KCl to either of the above solutions decreases the phosphoenzyme level by 35%. Levels at pH 7.0 were less than 0.10 in all cases. These levels are similar to literature values (Barrabin et al., 1984). These results were not affected by spin labeling.

Under all buffer conditions, the formation of the phosphoenzyme had little or no effect on the EPR spectra (see Figure 2) or the effective rotational correlation times calculated from

Table III: Effects of Nucleotides and Ca^{2+} [a]

	$-P_i$	$+P_i$
Ca	0.92 ± 0.08	
ADP	1.11 ± 0.10	0.87 ± 0.15
ADP, Ca	0.94 ± 0.08	1.02 ± 0.16
AMPPNP	1.02 ± 0.06	
AMPPNP, Ca	1.08 ± 0.12	
ATP, Ca (SS)	1.1 ± 0.5	
ATP, Ca (TR)	1.03 ± 0.07	

[a] Values shown are τ_r/τ_{r0} (see Materials and Methods), where τ_r and τ_{r0} are the effective rotational correlation times (from ST-EPR) in the presence and absence of the ligands indicated at left (except ATP and calcium, which was compared to the same experiment without ATP). All experiments were performed in SRB, plus the indicated ligands, at final concentrations of 0.45 mM Ca^{2+}, 5 mM ADP, 5 mM P_i, and 5 mM AMPPNP. The steady-state ATP experiment (SS) was performed in SRB with the addition of 30 mM imidazole, pH 7.4, 50 mM creatine phosphate, 1 μg of A23187/0.05 mg of SR protein, 0.45 mM $CaCl_2$, and creatine kinase to provide a 20-fold excess of activity over that of the Ca-ATPase. The central region of the ST-EPR spectrum was acquired within 10 min after addition of 5 mM ATP. The time-resolved (TR) experiment was performed with caged ATP as indicated in Figure 4. The uncertainty is the standard deviation for $n = 4$–6.

the ST-EPR spectra (Table II). There may be a slight decrease in the correlation time due to phosphoenzyme formation at 4 °C in the presence of DMSO, but (a) there was no significant effect of phosphate at 25 °C (see Table II), where phosphoenzyme formation is substantial, and (b) a similar decrease was also seen at pH 7.0 in the presence of 80 mM KCl (data not shown), where virtually no phosphoenzyme is formed. Therefore, the decrease is most likely due to nonspecific effects of phosphate, not to phosphorylation per se. We confirmed the result of Squier and Thomas (1988) that DMSO causes about a 2-fold increase in the effective correlation time even in the absence of phosphate. DMSO has been proposed to stabilize the E_2 state and thus enhance phosphoenzyme formation, whereas micromolar calcium should promote the E_1 state and destabilize the phosphoenzyme (de Meis et al., 1980). Micromolar Ca^{2+} caused no significant change in either the conventional or ST-EPR spectrum (data not shown), whether 40% DMSO was present or not, suggesting that there is no difference in the microsecond dynamics between the E_1 and E_2 states.

Effects of Nucleotides and Calcium. Nonhydrolyzable nucleotides (ADP and AMPPNP) and calcium were added to mimic the E_1 states that are proposed to occur prior to the proposed translocation step. Calcium and AMPPNP were at standard concentrations (Inesi & de Meis, 1985; Martonosi & Beeler, 1983). ADP was used with and without inorganic phosphate as a control for the other ligands, since ADP and P_i do not bind tightly to E_1 states prior to the proposed translocation step; ADP should bind tightly only to the phosphoenzyme in the proposed $E_1 \sim P \cdot Ca_2$ state (obtained only under transient conditions), and P_i should bind tightly only to the proposed E_2 state, under phosphoenzyme-promoting conditions. The conventional EPR spectra show no change upon ligand addition (Figure 3). Therefore, any changes observed in the ST-EPR spectra must be due to changes in the microsecond mobility of the protein. The addition of Ca (micromolar), AMPPNP, AMPPNP/Ca, ADP, ADP/Ca, ADP/Ca/P_i, and ADP/P_i had no significant effect on the ST-EPR spectra (see Figure 3 and Table III), indicating that the $E_1 \cdot Ca_2$, $E_1 \cdot Ca_2 \cdot$nucleotide, and $E_1 \cdot$nucleotide states are indistinguishable from the resulting enzyme in microsecond protein rotational mobility.

Steady-State ATP Hydrolysis. In order to investigate the proposed translocation step (from $E_1 \sim P \cdot Ca_2$ to $E_2 \cdot P \cdot Ca_2$), the

NUCLEOTIDES/Ca-ENZYME
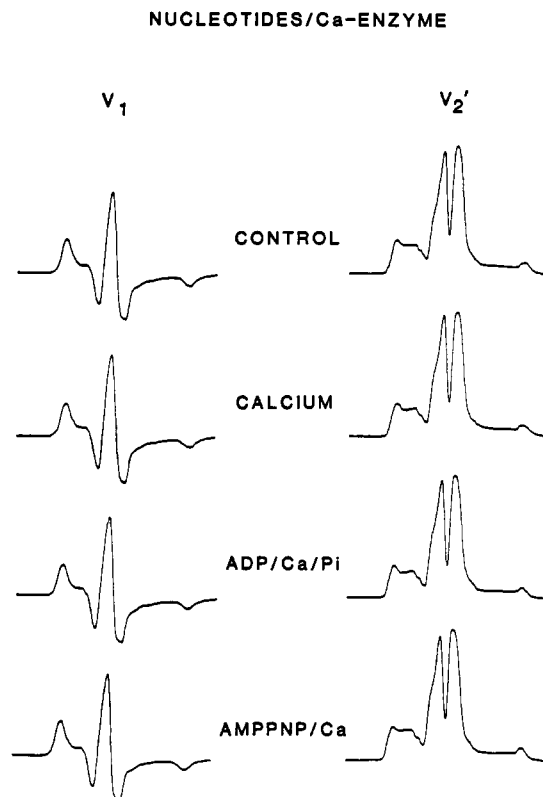

FIGURE 3: Effects of nucleotides and calcium on EPR spectra of MSL-Ca-ATPase. Left: conventional (V_1) EPR spectra. Right: saturation-transfer EPR (V_2') spectra. All solutions contained SRB plus the following, as indicated: 0.45 mM $CaCl_2$, 5 mM ADP, 5 mM P_i, and 5 mM AMPPNP. Spectra were recorded at 4 °C. The baseline is 110 G wide.

enzyme was monitored during Ca-dependent ATP hydrolysis. At high (100 mM) KCl, this transition has been proposed to be rate-limiting, so that $E_1 \sim P \cdot Ca_2$ should be predominant (Shigekawa et al., 1978; Shigekawa & Dougherty, 1978a,b). At low (<10 mM) KCl, $E_2 \cdot P \cdot Ca_2$ should be predominant (Shigekawa et al., 1978; Shigekawa & Dougherty, 1978a,b). The experiments of Shigekawa and co-workers were performed between 0 and 10 °C. The ATPase activity at 4 °C is approximately $^1/_{20}$ the rate at 25 °C. However, at the high protein concentrations used in EPR, 5 mM ATP is hydrolyzed in less than 2 min, which is not enough time to mix the sample, tune the spectrometer, and record the signal. Therefore, 50 mM creatine phosphate plus creatine kinase was used to regenerate the ATP. Under these conditions, the enzyme undergoes steady-state hydrolysis for 10–15 min at 4 °C, enough time to obtain acceptable ST-EPR data.

C'/C (an ST-EPR parameter sensitive to microsecond rotational motion) was measured under these steady-state ATP hydrolysis conditions (spectra not shown). The effective correlation time during ATP hydrolysis was not significantly different (no more than a 50% change) from that of a control without ATP (see Table III, bottom). The large uncertainty is due to the short time available for mixing, inserting the sample, tuning the instrument, and recording the data. The effective correlation time was essentially the same after steady-state activity as before ATP addition, indicating that the hydrolytic products (ADP and phosphate) do not affect the microsecond protein mobility. This is in agreement with the nucleotide results (Table III).

ATPase Activity Inhibited by Vanadate. The effects of ATP and Ca were also studied in the presence of vanadate. The V_1 spectra showed no changes, indicating that there are
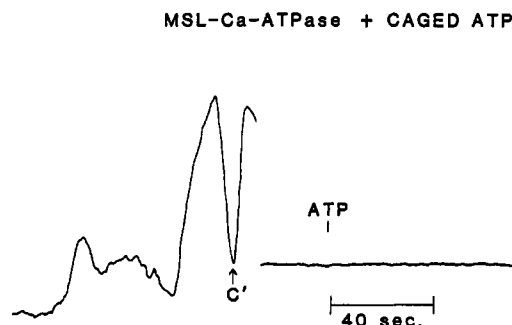
MSL-Ca-ATPase + CAGED ATP

FIGURE 4: Saturation-transfer EPR spectra of the MSL-Ca-ATPase during active Ca-ATPase cycling induced by photolysis of caged ATP. Left: First 50 G of the ST-EPR spectrum in SRB with 0.45 mM CaCl$_2$, 1 μg of A23187/0.05 mg of SR protein, and 5 mM caged ATP. Right: C' vs time, with a time resolution (filter time constant) of 2.0 s. ATP (1–1.5 mM) was released by the laser pulse at the indicated point. No significant effects of the laser flash were observed when the experiment was carried out in the absence of caged ATP. The temperature was 4 °C.

no charges in nanosecond motion. Monovanadate had no effect of the V_2' parameters. In SRB with 5 mM ATP, decavanadate increased the effective correlation times by 49 ± 9% in the absence of Ca^{2+} and by 30 ± 11% in the presence of 0.45 mM Ca^{2+}. Similar results were obtained with ADP.

Transient ATP Hydrolysis Induced by Photolysis of Caged ATP. In order to (a) obtain higher precision in measuring protein dynamics during the steady-state phase of the Ca-ATPase cycle and (b) investigate whether there are changes in the transient phase that are not observed in the steady state, ST-EPR was detected before and after flash photolysis of caged ATP. Upon exposure to light (UV light from an excimer laser), caged ATP releases ATP (Kaplan et al., 1978; McCray et al., 1980). The EPR sample can be mixed with caged ATP in the dark and then monitored before and immediately after ATP release (Berger et al., 1989; Fajer et al., 1990; Ostap & Thomas, 1991). Sensitivity and precision are much better than in experiments using ATP (described above), since precise sample insertion and tuning can occur before photolysis. Transient changes can be detected with a time resolution of about 1 s. In the present study, typically 1 mM ATP was produced from 5 mM caged ATP (as assayed by the liberated phosphate after the experiment, compared to an unexposed control). The ATPase activity 5 min after the experiment was inhibited no more than 12%.

As shown in Figure 4, the fixed spectral position C' was scanned versus time. This spectral position is very sensitive to changes in microsecond mobility. The arrow indicates the time of the laser pulse and thus the release of ATP. There is no significant effect of ATP. In seven trials, the maximum increase in C' due to the flash (measured 5 s after the flash) was +0.008 ± 0.018 (SEM), corresponding to an insignificant increase in the effective rotational correlation time (+3% ± 7%) due to ATP. Similarly, there were no significant changes due to a laser flash in the absence of protein but the presence of ATP. Therefore, there are no transient changes in microsecond protein rotational mobility during Ca-dependent ATP hydrolysis on a time scale greater than 1 s after ATP release.

DISCUSSION

The general question posed by the present study is whether any changes in microsecond rotational motion of the Ca-ATPase occur during the enzymatic cycle, which is depicted in Scheme I [reviewed by Inesi and de Meis (1985)]. The principal feature of this model is that the Ca-ATPase can exist

Scheme I: Proposed Ca-ATPase Kinetic Cycle
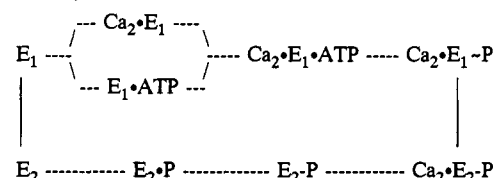
in two fundamentally different conformations that are energetically important, one (E$_1$) that has high calcium affinity but forms a weak (high-energy) phosphoenzyme bond and another (E$_2$) that has low calcium affinity but a more stable phosphoenzyme. Specifically, we are asking whether different mobilities are associated with specific states in the cycle, as mimicked by ligand binding under equilibrium conditions or as detected directly during active enzyme cycling.

Effects of Cross-Linking and Decavanadate. We have previously shown that ST-EPR spectra of MSL-Ca-ATPase are sensitive to protein–protein interactions produced by decavanadate (Lewis & Thomas, 1986) and by interprotein cross-linking (Squier et al., 1988). In the present study, we have shown that treatment with both cross-linking and decavanadate decreases the protein mobility more than either treatment alone (Figure 1, Table I). This result confirms the principle that ST-EPR is sensitive to protein–protein associations in this system but also indicates that residual microsecond protein rotational motion is still present when only one agent is used. This could be due to motions of the entire Ca-ATPase within the decavanadate-induced crystalline array or to large-scale segmental flexibility within the Ca-ATPase (Lewis & Thomas, 1986; Horvath et al., 1990). It has been proposed that decavanadate binding, which induces the formation of an ordered array of Ca-ATPase dimers (Buhle et al., 1983; Taylor et al., 1984), converts the enzyme into an analogue of the E$_2$-P state. Since arrays of monomers are formed under conditions proposed to mimic the E$_1$ state (Dux et al., 1985), it is plausible that the E$_1 \rightarrow$ E$_2$ (or Ca$_2$·E$_1 \sim$P $\rightarrow$ Ca$_2$·E$_2$-P) transition involves a monomer–dimer transition. Therefore, it is important to test whether decavanadate really induces an analogue of E$_2$-P.

Effects of Phosphoenzyme Formation or Monovanadate. The formation of phosphoenzyme (probably corresponding to E$_2$-P in Scheme I) from inorganic phosphate does not significantly change the microsecond protein rotational mobility (Figure 2, Table II), which is quite sensitive to protein association. Thus, E$_2$-P formation does not result in dimerization of the enzyme. Monovanadate also has a negligible effect on protein mobility (Lewis & Thomas, 1986), suggesting that monovanadate is a better phosphate analogue than is decavanadate. The effect obtained with decavanadate (Table I) could represent protein–protein interactions not normally found in the Ca-ATPase cycle or interactions that are present in other states in the cycle, which can only be observed in the presence of ATP and Ca^{2+}. In a complementary study using fluorescence resonance energy transfer (Birmachu et al., 1989), it was found that neither monovanadate nor decavanadate nor inorganic phosphate changed the distance between the IAE-DANS and FITC sites in the Ca-ATPase, suggesting a lack of change in the internal structure of the monomer. These results suggest that the transition from E$_1$ to E$_2$-P does not involve a substantial change in the overall shape, flexibility, oligomeric state, or internal structure of the Ca-ATPase.

We confirm that DMSO, which promotes phosphoenzyme formation, decreases the microsecond rational mobility of the Ca-ATPase (Table II) (Squier & Thomas, 1988), consistent

with previous reports that nonaqueous solvents such as DMSO produce protein aggregates detectable in electron micrographs (Van Winkle et al., 1985). However, no further effect is observed upon phosphate addition (Table II), showing that phosphoenzyme formation in the absence of calcium does not induce protein aggregation. It remains true that protein aggregation (induced by DMSO or other perturbations) inhibits phosphoenzyme decomposition in the presence of calcium (Squier & Thomas, 1988), but the aggregation states and phosphoenzyme states do not appear to be tightly coupled.

Effects of Ca^{2+} and Nucleotides. The addition of calcium and nucleotides (ADP and AMPPNP) does not change the microsecond protein mobility (Figure 3, Table III). This suggests that the E_1 state is indistinguishable in overall shape, flexibility, and protein–protein interaction from the E_1·Ca$_2$ and the E_1·Ca$_2$·nucleotide states. This is in agreement with Inesi and Watanabe (1982), who showed that the distance between Ca-ATPase molecules did not change upon ATP and/or Ca addition. The addition of mono- or decavanadate to these E_1·X states and to the cycling enzyme produced results similar to those of vanadate alone. Monovanadate did not affect the microsecond mobility, whereas decavanadate decreased it. This decrease was less than that found for decavanadate alone, suggesting that calcium and/or nucleotides interfered with the decavanadate effect. This is in agreement with Dux and Martonosi (1983b), who found that nucleotides and calcium interfered with array formation.

Effects of Active Enzyme Cycling. It remains possible that changes in large-scale protein mobility occur during the Ca-ATPase cycle but can be observed only during active calcium transport, associated either with calcium translocation or with other steps that cannot be mimicked under equilibrium conditions. Indeed, one of the most important intermediates in the proposed cycle, E_1~P·Ca$_2$, cannot be isolated at equilibrium and thus must be studied during the active enzymatic cycle. Therefore, ST-EPR was performed in the presence of ATP and Ca, under conditions (low temperature, 0.1 M KCl) where E_1~P·Ca$_2$ is the predominant intermediate in the steady state, and E_2-P is probably also significantly populated (Shigekawa & Dougherty, 1978; Shigekawa et al., 1978 a,b). Photolysis of caged ATP permitted measurements in both the steady-state and transient phases of the reaction. No change in microsecond mobility (no more than a 10% change) was observed in the steady state (Table III, bottom), suggesting that no change in the oligomeric state or large-scale segmental flexibility of the protein occurs in the transport cycle. A remaining possibility is that the state with altered mobility is present only transiently and is not predominant during the steady state of the Ca-ATPase cycle. Therefore, we monitored the ST-EPR signal under transient conditions using caged ATP, allowing us to monitor the protein's mobility during the initial (pre-steady-state) part of the cycle, probably including the proposed translocation step, from E_1~P·Ca$_2$ to E_2-P·Ca$_2$ (Blasie et al., 1990; Alonso & Hecht, 1990). No changes in microsecond mobility were observed within the time resolution of 1 s (Figure 4), again indicating that no change in large-scale protein dynamics accompanies transport.

The lack of significant change (no more than 10%) in the effective correlation time due to various ligands, including those that produce active transport, indicates that there is no substantial change in the size or shape of the rotating unit in the membrane. In particular, a transition from a monomer to a dimer (or the reverse) is clearly ruled out, since the rotational correlation time is predicted to be proportional to the cross-sectional area of the rotating protein in the bilayer (Saffman

& Delbrück, 1975; Birmachu & Thomas, 1990), and this has been verified in ST-EPR studies of MSL-SR in which oligomer formation was induced by covalent cross-linking (Squier et al, 1988a).

Relationship to Other Spectroscopic Studies. Previous studies have shown a striking correlation between overall rotational dynamics of the Ca-ATPase and its enzymatic activity. ST-EPR studies of MSL-SR have shown that inhibition of Ca-ATPase activity consistently results from inhibition of microsecond rotations, whether due to reconstitution with solid lipids (Hidalgo et al., 1978), vanadate-induced crystallization (Lewis & Thomas, 1986), covalent cross-linking (Squire et al., 1988a), partial delipidation (Squier & Thomas, 1988), or solvent perturbation (Squier & Thomas, 1988). Conversely, activation of the Ca-ATPase with diethyl ether is accompanied by enhanced microsecond motion (Bigelow & Thomas, 1987). Taken together, these results indicate that overall rotational mobility, or at least the lack of aggregation, is essential for maximal Ca-ATPase activity. These results seem consistent with the proposal that changes in protein–protein association are integral to the Ca-ATPase cycle, which is further supported by the observation that decavanadate induces lateral association of the Ca-ATPase (Dux et al., 1985), with an accompanying decrease in protein rotational mobility (Lewis & Thomas, 1986). However, the present results show that this rotational mobility does not change upon the initiation of Ca-ATPase activity, implying that the essential protein motions are not tightly coupled to the enzymatic cycle.

The lack of effects on overall (microsecond) rotational mobility, detected with MSL, contrasts with effects observed on local (nanosecond) motion, detected with IASL. Nucleotides and vanadate both decreased the mobility (Coan & Inesi, 1977; Coan & Keating, 1983; Coan et al., 1986). By spectral subtractions, it was shown that the decrease in mobility represented a transition between two distinct conformational states (Lewis & Thomas, 1987). Except for the effects of decavanadate, the observed changes are probably localization to a small part of the protein, since similar conditions do not induce substantial global changes, as detected by long-range energy-transfer measurements (Birmachu et al., 1989) or ST-EPR (present study). Initiation of the active Ca-ATPase cycle, using photolysis of caged ATP as in the present study, produced EPR transients in IASL-SR that probably correspond to a transition between the two conformational states (Lewis & Thomas, 1987). Transient X-ray diffraction signals have been observed under similar conditions (Blasie et al., 1990). Thus structural changes are induced by initiation of the Ca-ATPase cycle, but the present study indicates that these changes do not involve substantial changes in the size, shape, oligomeric state, or lipid–protein interactions of the enzyme. The photolysis of caged compounds has also been used to detect EPR transients in solutions of contractile proteins (Berger et al., 1989; Ostap & Thomas, 1991) and in muscle fibers (Fajer et al., 1990). It is clear that spectroscopy using caged compounds is a powerful approach to detecting transients in molecular structure and dynamics, particularly in molecular assemblies that are not easily studied by rapid-mixing techniques.

Conclusions. We conclude that microsecond rotational motions of the Ca-ATPase do not change substantially under conditions that cause transitions among the principal intermediate states in the enzymatic cycle. Although previous studies have shown that protein rotational mobility is essential to the Ca-ATPase cycle and that restriction of this mobility by induced protein aggregation inhibits the cycle (Squier &

Thomas, 1988; Squier et al., 1988b; Birmachu & Thomas, 1990), these motions are not changed by it. The results from the caged ATP experiments indicate that substantial changes in protein mobility do not occur during the Ca-ATPase cycle unless they occur very early in the transient phase or at some later point in the cycle that is not significantly populated in the steady state. Future experiments involving higher time resolution, different solution conditions, or different caged compound (e.g., caged phosphate, caged calcium) are needed to resolve these remaining questions. Microsecond rotational mobility is quite sensitive to changes in the oligomeric state and large-scale flexibility of the Ca-ATPase (Squier et al., 1988; Birmachu & Thomas, 1990), so the present study indicates that these changes do not occur as part of the transport cycle. This does not exclude the possibility that small-scale rearrangements occur within an oligomeric unit, only that the size and shape of this oligomeric unit do not change substantially.

ACKNOWLEDGMENTS

REFERENCES

Andersen, J. P., & Vilsen, B. (1985) *FEBS Lett. 189*, 2847.

Andersen, J. P., Vilsen, B., Nielsen, H., & Moller, J. V. (1986) *Biochemistry 25*, 6439.

Barrabin, H., Scofano, H. M., & Inesi, G. (1984) *Biochemistry 23*, 1542.

Berger, C. L., Svensson, E. C., & Thomas, D. D. (1989) *Proc. Natl. Acad. Sci. U.S.A. 86*, 8753–8757.

Bigelow, D. J., & Thomas, D. D. (1987) *J. Biol. Chem. 262*, 13449–13456.

Bigelow, D. J., Squier, T. C., & Thomas, D. D. (1986) *Biochemistry 25*, 194.

Birmachu, W., & Thomas, D. D. (1990) *Biochemistry 29*, 3904.

Birmachu, W., Nisswandt, F. L., & Thomas, D. D. (1989) *Biochemistry 28*, 3940.

Buhle, E. L., Knox, B. E., Serpersu, E., & Aebi, U. (1983) *J. Ultrastruct. Res. 85*, 186.

Chen, P. S., Toribara, T. Y., & Warner, H. (1956) *Anal. Chem. 28*, 1756.

Coan, C. R., & Inesi, G. (1977) *J. Biol. Chem. 252*, 3044.

Coan, C., & Keating, S. (1983) *Biochemistry 21*, 3214.

Coan, C., Scales, D. J., & Murphy, A. J. (1986) *J. Biol. Chem. 260*, 10394.

Deamer, D. W., & Baskin, R. J. (1969) *J. Cell Biol. 42*, 296.

de Meis, L., Martins, O. B., & Alves, E. W. (1980) *Biochemistry 19*, 4252.

Dupont, Y., & Bennett, N. (1982) *FEBS Lett. 139*, 237.

Dux, L., & Martonosi, A. (1983a) *J. Biol. Chem. 258*, 2599.

Dux, L., & Martonosi, A. (1983b) *J. Biol. Chem. 258*, 11896.

Dux, L., Taylor, K. A., Ting-Beall, H. P., & Martonosi, A. (1985) *J. Biol. Chem. 260*, 11730.

Fagan, M. H., & Dewey, T. G. (1986) *J. Biol. Chem. 261*, 3654.

Fajer, P. G., Fajer, E. A., & Thomas, D. D. (1990) *Proc. Natl. Acad. Sci. U.S.A. 86*, 5538.

Fernandez, J. L., Rosemblatt, M., & Hidalgo, C. (1980) *Biochim. Biophys. Acta 599*, 552.

Froehlich, J., & Taylor, E. (1976) *J. Biol. Chem. 251*, 2307.

Froehlich, J. P., & Heller, P. F. (1985) *Biochemistry 24*, 126.

Gornall, A. G., Bardawill, C. J., & David, M. M. (1949) *J. Biol. Chem. 177*, 751.

Hidalgo, C., & Thomas, D. D. (1977) *Biochem. Biophys. Res. Commun. 78*, 1175.

Hidalgo, C., Thomas, D. D., & Ikemoto, N. (1978) *J. Biol. Chem. 253*, 6879.

Highsmith, S., & Cohen, J. A. (1987) *Biochemistry 26*, 154.

Horvath, L. I., Dux, L., Hankovszky, H. O., Hideg, K., & Marsh, D. (1990) *Biophys. J. 58*, 231.

Hymel, L., Maurer, A., Berenski, C., Jung, C. Y., & Fleischer, S. (1984) *J. Biol. Chem. 259*, 4890.

Inesi, G., & Watanabe, T. (1982) *Biochemistry 21*, 3254.

Inesi, G., & de Meis, L. (1985) in *The Enzymes of Biological Membranes* (Martonosi, A. N., Ed.) Vol. 3, pp 157–191, Plenum Press, New York.

Jilka, R. L., Martonosi, A. N., & Tillack, T. W. (1975) *J. Biol. Chem. 250*, 7511.

Kaplan, J. H., Forbush, G., III, & Hoffman, J. F. (1978) *Biochemistry 17*, 1929.

Kurobe, Y., Nelson, R. W., & Ikemoto, N. (1983) *J. Biol. Chem. 258*, 4381.

Laemmli, U. K. (1970) *Nature (London) 277*, 680.

Lanzetta, P. A., Alvarez, L. J., Reinsch, P. S., & Candia, O. A. (1979) *Anal. Biochem. 100*, 95.

Lewis, S. M., & Thomas, D. D. (1986) *Biochemistry 25*, 4615.

Lewis, S. M., & Thomas, D. D. (1987) *Biophys. J. 51*, 403a.

Markus, S., Priel, A., & Chipman, D. M. (1989) *Biochemistry 28*, 793.

Martonosi, A. N., & Beeler, T. G. (1983) in *Handbook of Physiology—Section 10: Skeletal Muscle* (Peachey, L. D., Adrian, R. H., & Geiger, S. R., Eds.) pp 417-485, American Physiological Society, Bethesda, MD.

Martonosi, A. N., Jona, I., Molnar, E., Seidler, N. W., Buchet, R., & Varge, S. (1990) *FEBS Lett. 268*, 365–370.

Maurer, A., & Fleischer, S. (1984) *J. Bioenerg. Biomembr. 16*, 491.

McCray, J. A., Herbette, L., Kihara, T., & Trentham, D. R. (1980) *Proc. Natl. Acad. Sci. U.S.A. 77*, 7237.

McIntosh, D. B., & Ross, D. C. (1988) *J. Biol. Chem. 263*, 12220.

Moller, J. V., Andersen, J. P., & LeMarie, M. (1982) *Mol. Cell. Biochem. 42*, 83.

Napolitano, C. A., Cooke, P., Segalman, K., & Herbette, L. (1983) *Biophys. J. 42*, 119.

O'Neal, S. G., Rhoads, D. B., & Racker, E. (1979) *Biochem. Biophys. Res. Commun. 89*, 845.

Ortiz, A., Garcia-Carmona, F., Garcia-Canovas, F., & Gomez-Fernandez, J. (1984) *Biochem. J. 221*, 213.

Ostap, M. O., & Thomas, D. D. (1991) *Biophys. J.* (in press).

Papp, S., Kracke, G., Joshi, N., & Martonosi, A. (1986) *Biophys. J. 49*, 411.

Papp, S., Pikula, S., & Martonosi, A. (1987) *Biophys. J. 51*, 205.

Scales, D., & Inesi, G. (1976) *Biophys. J. 16*, 735.

Shigekawa, M., & Dougherty, J. P. (1978a) *J. Biol. Chem. 253*, 1451.

Shigekawa, M., & Dougherty, J. P. (1978b) *J. Biol. Chem. 253*, 1458.

Shigekawa, M., Dougherty, J. P., & Katz, A. M. (1978) *J. Biol. Chem. 253*, 1442.

Squier, T. C., & Thomas, D. D. (1986a) *Biophys. J. 49*, 921.

Squier, T. C., & Thomas, D. D. (1986b) *Biophys. J. 49*, 936.

Squier, T. C., & Thomas, D. D. (1988) *J. Biol. Chem. 263*, 9171.

Squier, T. C., Bigelow, D. J., & Thomas, D. D. (1988a) *J. Biol. Chem. 263*, 9178.

Squier, T. C., Hughes, S. E., & Thomas, D. D. (1988b) *J. Biol. Chem. 263*, 9162.

Taylor, K., Dux, L., & Martonosi, A. (1984) *J. Mol. Biol. 174*, 193.

Thomas, D. D. (1986) in *Techniques for Analysis of Membrane Proteins* (Ragan, I., & Cherry, R., Eds.) pp 377–431, Chapman & Hall, London.

Thomas, D. D., & Hidalgo, C. (1978) *Proc. Natl. Acad. Sci. U.S.A. 75*, 5488.

Thomas, D. D., Bigelow, D. J., Squier, T. C., & Hidalgo, C. (1982) *Biophys. J. 37*, 217.

Vanderkooi, J. M., Ierokomos, A., Nakamura, H., & Martonosi, A. (1977) *Biochemistry 16*, 1262.

Van Winkle, W. B., Bick, R. J., Tate, C. A., & Entman, M. L. (1985) *Biophys. J. 47*, 284a.

Varga, S., Csermely, P., & Martonosi, A. (1985) *Eur. J. Biochem. 148*, 119.

Volpe, P., Damiani, E., Maurer, A., & Tu, A. T. (1986) *Arch. Biochem. Biophys. 246*, 90.

Wang, T. (1986) *J. Biol. Chem. 261*, 6307.

Watanabe, T., Lewis, D., Nakamoto, R., Kurzmack, M., Fronticelli, C., & Inesi, G. (1981) *Biochemistry 20*, 6617.

Yantorno, R. E., Yamamoto, T., & Tonomura, Y. (1963) *J. Biochem. (Tokyo) 94*, 1137.

Probing the Relationship between α-Helix Formation and Calcium Affinity in Troponin C: ¹H NMR Studies of Calcium Binding to Synthetic and Variant Site III Helix–Loop–Helix Peptides[†]

Gary S. Shaw, Robert S. Hodges, and Brian D. Sykes*

Department of Biochemistry and MRC Group in Protein Structure and Function, University of Alberta, Edmonton, Alberta T6G 2H7, Canada

ABSTRACT: Three 34-residue peptides corresponding to the high-affinity calcium-binding site III and two variant sequences from the muscle protein troponin C (TnC) were synthesized by solid-phase techniques. The two variant 34-residue peptides had amino acid modifications at either the coordinating positions or both the coordinating and noncoordinating positions, which corresponded to the residues found in the low-affinity calcium-binding site II of TnC. High-field ¹H NMR spectroscopy was used to monitor calcium binding to each peptide to determine the effect these amino acid substitutions had on calcium affinity. The dissociation constant of the native site III peptide (SCIII) was 3×10^{-6} M, smaller than that of the peptide incorporating the ligands from site II (LIIL), 8×10^{-6} M, and that with the entire site II loop (LII), 3×10^{-3} M, which bound calcium very weakly. These calcium dissociation constants demonstrate that very minor amino acid substitutions have a significant effect on the dissociation constant and give some insight into why the dissociation constants for site III and IV in TnC are 100-fold smaller than those for sites I and II. The results suggest that the differences in coordinating ligands between sites II and III have very little effect on Ca²⁺ affinity and that the noncoordinating residues in the site II loop are responsible for the low affinity of site II compared to the high affinity of site III in TnC.

Calcium-binding proteins comprise a large class of regulatory proteins that contain between one and four highly conserved metal-ion binding sites. In many cases the trademark of these calcium-binding sites is a contiguous sequence of about 30 amino acids that forms a helix–loop–helix structural motif upon binding of calcium (Kretsinger & Nockolds, 1973). Coordination of the metal ion in these proteins occurs in a 12-residue loop region where calcium is ligated to the carboxyl, amide, or hydroxyl side chains of five amino acid residues at positions 1 (X), 3 (Y), 5 (Z), 9 (–X), and 12 (–Z) and to the main-chain carbonyl of the residue at position 7 (–Y). These residues form a pentagonal bipyramid arrangement about the calcium ion in which the carboxylate side chain of the residue at position –Z chelates the metal in a bidentate fashion (Strynadka & James, 1989).

Recently, a detailed analysis of all available amino acid sequences for calcium-binding proteins that have contiguous calcium-binding loops was compiled in an effort to determine a preference for amino acids at various positions of the loop (Marsden et al., 1990). It was found that for the 12 loop positions the only invariant amino acids existed at positions 1, 6, and 12 where aspartic acid, glycine, and glutamic acid residues, respectively, are highly favored (>85%). As the calcium affinity of a calcium-binding protein is most likely a function of the composition of the calcium-binding loop, the variability of the nine positions in the calcium-binding loops is consistent with the dramatic range of calcium affinities within the family of calcium-binding proteins. For example, parvalbumin has one of the highest measured calcium affinities [$K_d \approx 10^{-9}$ M, Goodman et al. (1979)] while some aequorin proteins can have a calcium affinity that is several orders of